Water Practice & Technology

IWA PUBLISHING

Water Practice & Technology Vol 18 No 5, 1074 doi: 10.2166/wpt.2023.066

Zirconium fumarate metal-organic framework: a selective adsorbent for fluoride from industrial wastewater

Ranjana Kumari[a], Anil Kumar[a], Supriya Sarkar[b], Tamal Kanti Ghosh[b] and Subhankar Basu[a,*]

[a] Department of Applied Sciences and Humanities, National Institute of Advanced Manufacturing Technology (NIAMT) Ranchi, Jharkhand 834003, India
[b] Environment Research Group, Tata Steel Limited, Jamshedpur 831007, India
*Corresponding author. E-mail: subhankarb@niamt.ac.in

SB, 0000-0002-5764-9965

ABSTRACT

Many industrial processes produce high fluoride (150–450 mg/L) containing effluent. It may be recovered from the processing plants at the source. One effective technology is selective fluoride adsorption from the waste stream. Metal-organic frameworks (MOFs) are crystalline compounds with high surface area, pore volume, and tuneable pore channels and are suitable adsorbents. This study used zirconium fumarate (ZrFu) MOF to recover the fluoride from iron and steel industrial wastewater collected from blast furnaces and coke plants, respectively. In batch experiments, complete fluoride uptake from synthetic water (150 mg F/L) was obtained with 3 g ZrFu/L ($q_e = 49.66$ mg/g), while for blast furnace (170 mg F/L) and coke plant (130 mg F/L) wastewater, 10 g ZrFu/L was required, ($q_e = 17$ mg/g) and ($q_e = 13$ mg/g), respectively. This difference in adsorbent dose was caused by interfering ions in industrial wastewater, which compete for the same adsorption sites as fluoride ions. Chemisorption was the rate-limiting step, and it conforms to the Langmuir isotherm and the pseudo-second-order model. Fluoride desorption was achieved in deionized water in 1 h. This suggests that the adsorption–desorption process could be scaled up to an industrial process to recover and reuse fluoride from wastewater.

Key words: high surface area, iron and steel industry, porous materials, recover and reuse, wastewater

HIGHLIGHTS

- Zirconium fumarate (ZrFu) with a high surface area was prepared.
- Selective fluoride adsorption from industrial wastewater was studied.
- Complete uptake of fluoride was obtained.
- The mechanism of fluoride adsorption is the ion-exchange process.
- Fluoride recovery was possible through adsorption–desorption processes.

1. INTRODUCTION

Fluoride is one of the reactive non-metallic elements. It combines directly or indirectly with many other elements and generates various fluoride compounds. Most fluoride compounds are stable and generally dissolve in nature. So fluoride remains in the surrounding environment (Loganathan *et al.* 2013; Halla *et al.* 2015). Fluoride originates from various sources, such as daily-use products (e.g., dental products, dietary supplements, and beverages), geogenic sources, and industrial production. The fluoride concentration in industrial wastewater is the highest among the different sources of origin, and the pollution level is also high (100–10,000 mg/L) (Wan *et al.* 2021).

The iron and steel industry, aluminium electrolysis, lead, aluminium, zinc, and copper smelting, rare earth element separation, uranium enrichment, photovoltaic industry, lithium-ion battery industry, cement industry, and thermal power generation are all fluoride-releasing industries (Wan *et al.* 2021). In the iron and steel industry, fluoride is present in iron smelting, waste gas, wastewater, and slag generated during ore mining, beneficiation, sintering, and smelting, which are essential for steel manufacturing by using a blast furnace. The high-temperature process in steelmaking releases potassium fluoride, sodium fluoride, and other fluoride compounds (Wan *et al.* 2021). Similarly, metallurgical industries, e.g., copper, zinc, aluminium smelting, etc., generate fluoride in the

wastewater. High fluoride-containing wastewater (10,000 mg/L) in copper smelting is challenging to treat (Castillo *et al.* 2020). In the zinc smelting process, fluoride comes from zinc concentrate electrolytes (1,000 mg/L) (Menad *et al.* 2003). A tonne of aluminium requires 30 kg of fluoride to be produced (Shan & Guo 2013). Photovoltaic solar panels generate 1,000–3,500 mg/L fluoride-containing wastewater (Drouiche *et al.* 2007). In the battery industry, hydrofluoric acid contributes to fluoride in wastewater (500 mg/L) (Drouiche *et al.* 2012). Other industrial processes resulting in fluoride wastewater include uranium enrichment, phosphate fertilizer production, and ceramic, and cement factories (Dehghani *et al.* 2016).

Physical processes reduce the concentration, but not sufficiently to bring it down to the discharge standard (15 mg/L) (Schedule-VI, Central Pollution Control Board, India, The Environmental Protection Rules, 1986). Treatment of such high fluoride concentrations in industrial wastewater by physical (e.g., adsorption, membrane process) or chemical processes is also difficult (Wu *et al.* 2017). A literature review shows that various techniques have been reported to treat industrial wastewater with high fluoride concentrations. It can be divided into two categories: (i) chemical processes (such as chemical precipitation and coagulation/electro-coagulation) and (ii) physical processes (such as reverse osmosis (RO), ion-exchange (IX), electrodialysis, and adsorption) (Mohapatra *et al.* 2009). Fluoride-containing wastewater from the solar cell manufacturing process (Joint National Egyptian Chinese Renewable Laboratory, Egypt) was treated by chemical precipitation with quick lime and potassium hydroxide (Diwani *et al.* 2022). Hydrated lime was used for the separation of fluoride in wastewater from the fertilizer industry (Zueva *et al.* 2020). However, chemical precipitation is slow, and it is not efficient to reduce the fluoride concentration up to the discharge limit. Coagulation and chemical precipitation of fluoride produced in the microelectronics industry for wastewater treatment have been reported (Chang & Liu 2007). Similar high fluoride removal was reported in the electro-coagulation process with aluminium electrodes for treating steel industry wastewater (Mobarake Steel Complex, Esfahan, Iran) (Khatibikamal *et al.* 2010). In the electro-coagulation method, energy consumption and equipment costs are relatively high. Also, the selectivity of electrodes gets reduced frequently. Chemical precipitation and coagulation are the traditional methods of fluoride removal from waste streams (Khatibikamal *et al.* 2010). However, during precipitation and chemical coagulation processes, a large amount of chemicals is added, resulting in a high amount of fluoride precipitate sludge daily (Wan *et al.* 2021). Further, membrane technology can reduce fluoride in a wide pH range (Waghmare & Arfin 2015). The hybrid lime and RO system used for wastewater treatment at the aluminium fluoride manufacturing plant was reported to be efficient (Ezzeddine *et al.* 2015). However, treating high-strength and high-salinity wastewater is difficult, as membranes are frequently fouled (Singh *et al.* 2013). The coagulation-ultrafiltration process was studied for fluoride removal from wastewater generated in Shanghai, China's semiconductor manufacturing industry (Qiu *et al.* 2022). However, this process requires a large amount of coagulant. Ion-exchange technology reported up to 90–95% fluoride removal (Meenakshi 2006). However, other ions such as phosphate, sulphate, and bicarbonates in industrial wastewater lower its efficiency. Thus, chemical precipitation, coagulation, membrane processing, and ion-exchange resin used to reduce the fluoride content in the effluent are applicable only for low fluoride concentrations, as they are expensive (Singh *et al.* 2013). Also, in some cases, it has a low fluoride uptake capacity (Wan *et al.* 2021).

Among all the processes mentioned above, the adsorption process is considered one of the most promising methods for fluoride uptake because of its high uptake capacity, easy operating conditions, low operational cost, absence of harmful by-products, and low energy consumption (Patel *et al.* 2016; Dhanasekaran *et al.* 2017). In a recent study, calcium and zirconium modified acid-activated alumina (CAZ) reported 92% fluoride uptake (Kumari *et al.* 2020). Similarly, sulphuric acid-activated modified alumina resulted in 94% fluoride uptake from aluminium industry wastewater (National Aluminium Company Limited, Orissa, India) (Kumari *et al.* 2019). Drinking water treatment residues (polyaluminium chloride used as a coagulant) based on adsorptive material used for the treatment of industrial wastewater (smelting factory, Gyeonggi-do, South Korea) reported 90% fluoride uptake (Jung *et al.* 2016). The integrated process of calcium hydroxide precipitation and adsorption on hydroxyapatite was also reported to treat fluoride-containing wastewater from the aluminium finishing industry (Xanthi, Greece) (Melidis 2015). Alumina-modified citric acid showed fluoride uptake of 99% from phosphogypsum slag yard mine leachates (Li *et al.* 2022). These adsorbents show high uptake capacity, but no study on the adsorption–desorption process has been reported.

Metal-organic frameworks (MOFs) have received a lot of attention in recent years for their high fluoride adsorption due to their controllable pore structure, high stability, large surface area, and good physical and chemical properties (Ma & Zhou 2010; Li *et al.* 2011; DeCoste & Peterson 2014). Their uniform surface

structure, comparatively high void ratio, and outstanding chemical and thermal stability make them different from other inorganic porous materials (Eddaoudi *et al.* 2002; Furukawa *et al.* 2013). As a super fluoride adsorbent, aluminium fumarate (AlFu) MOF was reported; it has a large specific surface area (1,156 m^2/g) and higher uptake capacity (600 mg/g at 25 °C) than previously reported and commercially available water-stable MOFs (*Basolite*®-MOFs, Merck) (Karmakar *et al.* 2016). Reuse of AlFu MOF has been reported (Kumari *et al.* 2022). Similarly, MIL-96(Al) MOF showed high selectivity towards fluoride ions and high pH stability (3–10), with an adsorption capacity of 32 mg/g at 25 °C (Zhang *et al.* 2014). MOF-801, a zirconium-based MOF, also demonstrated a high rate of fluoride adsorption capacity (Tan *et al.* 2020). Hydroxyapatite (HAp)-based layered lanthanum-benzene tricarboxylic acid-based MOFs (La-BTC MOFs) showed promising results for fluoride removal from water (Jeyaseelan *et al.* 2022). However, these MOFs as adsorbents were reported to have low initial fluoride concentrations (2–15 mg F/L) and were formulated with synthetic water.

Zirconium fumarate (ZrFu) MOF has been reported to be thermally, chemically, and water stable, having a large surface area and high fluoride adsorption capacity (Mukherjee *et al.* 2016). It was prepared from $ZrCl_4$ and fumaric acid as Zr_6O_4 $(–OH)_4$ $(fumarate)_6$ XH_2O. In addition, the presence of Zr-bound-OH groups in the structure improves fluoride adsorption by the ion-exchange process. It has been found effective for fluoride removal in drinking water. But no study has been done to see if fluoride can be selectively separated from industrial wastewater at its source and then reclaimed for use by desorption. This has motivated us to prepare materials suitable for removing fluoride from industrial wastewater. The efficacy of ZrFu MOF as an adsorbent for selective fluoride recovery from industrial wastewater has been prepared and studied. The wastewater was collected from the clarifier tank of the coke plant and blast furnace at the Tata Steel Plant, Jamshedpur, India. Every tonne of steel produced requires 25 m^3 of water, and the rate of effluent generation is 5 m^3/h (Mukherjee *et al.* 2016). The wastewater is treated by primary, secondary (biological process), and tertiary (advanced oxidation process) treatment processes, respectively. Fluoride, chloride, nitrate, phosphate, total solids, total dissolved solids, and salinity are all present in high concentrations in the treated water (Mukherjee *et al.* 2016). In this study, the effects of contact time, pH variation, adsorbent dose, initial concentration, adsorption kinetics, and isotherms were studied with synthetic water to understand the adsorption mechanism and factors affecting the adsorption process. The MOF was then studied for industrial wastewater under optimized conditions. A simultaneous adsorption–desorption study was also carried out for the re-use of the material.

2. MATERIALS AND METHODS

2.1. Chemicals

Zirconium oxychloride octahydrate (98%) and fumaric acid (99.5%) were purchased from Loba Chemie Pvt. Ltd, India. *N*,*N*-Dimethyl formamide (DMF) (99%) and sodium fluoride (98%) were purchased from Merk Life Science Pvt. Ltd, India. Formic acid (85%) was purchased from Nice Chemical Pvt. Ltd, India. Ethanol (99.9%) was purchased from Changshu Hongsheng Fine Chemical Co., Ltd. The chemicals were used as-received.

2.2. Synthesis of ZrFu MOF

Zirconyl chloride octahydrate (1.6 g) and fumaric acid (0.58 g) were mixed with a mixed solvent to make ZrFu MOF. A mixed solvent was prepared by adding DMF (20 mL) and formic acid (7 mL). The mixture was filled in an autoclave (KLB Instruments Co. Pvt. Ltd, India), and it was heated at 130 °C for 6 h in a hot air oven (i-therm, Mumbai, India). The white-coloured precipitate was separated by centrifugation at 8,000 rpm for 20 min (REMI R-24, India). The MOF was washed at least three times with DMF followed by ethanol. Washed ZrFu MOF was dried at 105 °C for 1 day in a hot air oven and then mortar pestle into fine powder. The MOF was then dried at room temperature for 1 h in a vacuum oven (Stericox, Delhi, India) and stored for future use.

2.3. Adsorption–desorption study

The adsorption experiments were carried out in 500 mL plastic containers with 100 mL synthetic fluoride solutions ($C_o = 10$ mg/L). At 100 rpm, the experiments were carried out in an orbital shaker (Yorco Sales, Delhi, India). The effects of contact time (10–160 min), the effect of temperature (25–35 °C), the effect of adsorbent dose (0.3–2.0 g/L), the effect of pH (3–10), and the effect of initial fluoride concentration (5–30 mg/L) were studied. Fluoride levels in water were determined using a Fluoride Metre (Extech Instruments, FL700, USA). The fluoride removal efficiency and adsorption capacity were calculated by Equations (1) and (2) (Kumari *et al.* 2022).

Based on the experimental data, fluoride adsorption isotherms and kinetics were studied. The experiments were continued till adsorption equilibrium was achieved, after which there was no change in the fluoride uptake value with increasing the variable parameters mentioned above. An average of three sets of experimental data has been reported.

$$R(\%) = (1 - C_t/C_o) \times 100 \tag{1}$$

where R (%) denotes the fluoride uptake capacity of ZrFu MOF and C_o and C_t denote the initial and final fluoride concentrations in the solution, respectively.

$$q_e(\mathrm{mg/g}) = (C_o - C_e) \times V/m \tag{2}$$

where q_e is the amount of fluoride adsorbed per g of ZrFu MOF (mg/g); C_o and C_e are the initial and equilibrium concentrations of fluoride in the solution (mg/L) respectively, V is the volume of the solution (L), and m is the weight of ZrFu MOF (g).

Linear form of Langmuir and Freundlich isothermal models are in Equations (3) and (4) (Kumari *et al.* 2022)

$$C_e/q_e = 1/(q_m K_\mathrm{L}) + (1/q_m)C_e \tag{3}$$

$$\ln q_e = \ln K_\mathrm{F} + \ln C_e/n \tag{4}$$

where C_e is the solution's equilibrium fluoride concentration (mg/L), q_e is the amount of fluoride adsorbed per unit weight of ZrFu MOF (mg/g), q_m is the maximum uptake capacity (mg/g), and K_L is the Langmuir constant related to energy (L/mg).

Langmuir separation factor (R_L) was calculated by the following equation

$$R_\mathrm{L} = 1/(1 + K_\mathrm{L} C_o) \tag{5}$$

where C_o is the initial fluoride concentration, K_L is the Langmuir isotherm constant, and R_L is the dimensionless constant separation factor of the Langmuir isotherm.

After optimizing the operating conditions with synthetic water (150 mg/L), the adsorption study of ZrFu MOF for industrial wastewater was done. The experiments were carried out in 500 mL plastic containers containing 100 mL of synthetic fluoride solutions with compositions ranging from 10 to 150 mg/L (Mukherjee *et al.* 2016), an adsorbent dose of 1–5 g/L, and an adsorption time of 10–60 min. The tests were carried out in an orbital shaker set to a constant speed of 100 rpm ($T = 35$ °C and pH = 6). Wastewater was collected (January 2021) in a 10 L Jerry can from the clarifier of the coke plant (CP) and blast furnace (BF) of TATA Steel, Jamshedpur, India. The samples were centrifuged to remove the suspended solids, and the supernatant was used for the experiments. The wastewater was tested for chemical oxygen demand (COD), phosphate, chloride, nitrate, total hardness, and total solids using standard methods for water and wastewater analysis (American Public Health Association (APHA) *et al.* 1998). The pH was measured using a pH metre (LAB INDIA, Mumbai). The total solid was calculated using the gravimetric method. COD, chloride, and total hardness of the samples were estimated by the titration method. The nitrate and phosphate concentrations of the samples were determined by a UV–Vis spectrophotometer (Systronics 119, Mumbai). The fluoride desorption study was performed by adding 100 mL of DI water to the exhausted MOF. The mixture was shaken for 1 h at 100 rpm and 35 °C in a shake flask. The concentration of fluoride in the water was determined after the reaction. The regenerated MOF was again used in a fresh batch of synthetic and industrial wastewater. This process continued for several cycles for synthetic and industrial wastewater, respectively.

2.4. Characterization of MOFs

The structural characterization of the ZrFu MOF was conducted by an X-ray diffraction technique (XRD) using an X-ray diffractometer (Rigaku, Japan, Smart Lab 9Kw). Brunauer–Emmett–Teller (BET) analysis was performed at 77 K using a surface area analyser (Quantachrome Instruments, USA) to estimate the surface area, pore diameter, and pore volume of ZrFu MOF. The surface morphology of ZrFu MOF was analysed by a Field emission scanning microscope (FESEM; SM-6390LV, Jeol, Japan). The functional groups of the samples

before and adsorption studies were analysed using Fourier transform infrared (FTIR) spectroscopy (IR-Prestige 21, Shimadzu Corporation, Japan, IR-Prestige 21).

3. RESULTS AND DISCUSSION

3.1. Characterization of ZrFu MOF

The as-synthesized ZrFu MOF was characterized by XRD, surface area analyser and FESEM. The XRD pattern of the as-synthesized ZrFu MOF shows characteristic peaks that look similar (2Θ values) to MOF-801 reported earlier (Tan *et al.* 2020; Figure 1(a)). The XRD pattern reveals that the as-prepared MOF was highly crystalline and successfully synthesized. The surface area of as-prepared ZrFu MOF is 537.54 m^2/g, the pore volume is 0.229 cm^3/g, and the pore radius is 1.813 nm, according to BET analysis. The N_2 adsorption–desorption isotherm of ZrFu MOF shows typical type-I curves, which indicates that the micro-porous structure and the adsorption on the MOF is based on monolayer adsorption. The SEM image of ZrFu MOF shows a uniform morphology with octahedron particle shapes and particle sizes ranging from 90 to 100 nm (Figure 1(b)).

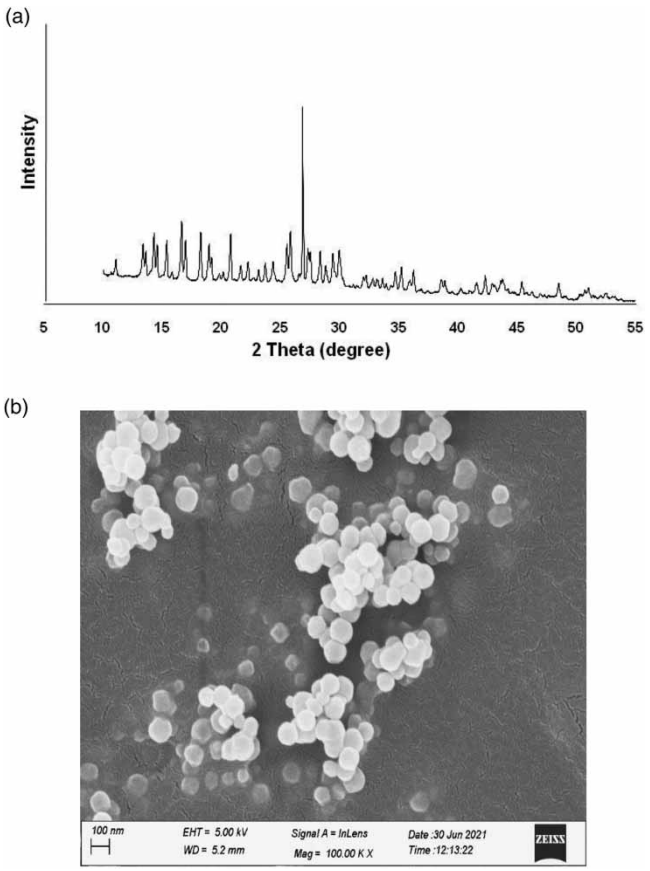

Figure 1 | XRD pattern (a) and SEM image of ZrFu MOF (b).

3.2. Factors affecting fluoride uptake capacity of ZrFu MOF

ZrFu MOF was chosen among some of the water-stable MOFs (MIL-96, AlFu, ZIF-8, ZIF-67, and CuBTC) because it showed complete fluoride uptake capacity under the given operating conditions (MOF dose of 1 g/L, $C_o = 10$ mg F/L, pH = 6, and $T = 35$ °C) (Supplementary Figure S1). The experiments were conducted in a shake flask. The study shows that the fluoride uptake capacity of the MOFs varies from one another. Under similar operating conditions, the ZrFu MOF showed 100% fluoride uptake compared to other studied MOFs. The variation in the MOFs adsorption could be due to differences in (i) electrostatic adsorption, (ii) complexation mechanisms (Zhu *et al.* 2018; Jeyaseelan *et al.* 2020), and (iii) surface area/volume ratio. Increased fluoride uptake capacity was observed in ZrFu MOF due to Zr^{+4} compared to Al^{+3}, Zn^{+2}, Co^{+2}, and Cu^{+2}. The positively charged higher valence ion (Zr) present in the synthesized MOF attracts more negatively charged fluoride ions by electrostatic attraction

and complexation (Zhu *et al.* 2018). The functional groups (e.g., carboxylate group, hydroxyl group) present on the MOF structure provide active sites for the adsorption of fluoride (Ke *et al.* 2018). Thus, ZrFu MOF was selected for further studies.

The reaction time to reach the adsorption equilibrium was determined to be from 10 to 160 min with an initial fluoride concentration of 10 mg/L. The fluoride uptake capacity was rapid at the initial stage, and then it continued to adsorb at a slower rate. The initial higher uptake of fluoride indicates that the fluoride ions occupied the readily available binding sites on the outer layer of the MOF. The slower fluoride uptake after 30 min was due to the slow diffusion of fluoride ions inside the micro-porous structure of ZrFu MOF (Dey *et al.* 2004). In this study, equilibrium was reached after 120 min of the reaction, and no change in the fluoride uptake was observed despite increasing the reaction time (Figure 2(a)). Similar results were obtained earlier (Mukherjee *et al.* 2016). The effect of pH on fluoride adsorption was studied (Figure 2(b)). The decrease in fluoride uptake capacity with increased pH was due to the electrostatic interaction between the ZrFu MOF and fluoride. Acidic pH facilitates protonation of the ZrFu MOF surface and consequently makes many positively charged active sites ($Zr–OH_2^+$) per unit area accessible. As a result, the fluoride uptake capacity increases at low pH due to electrostatic interaction between the positively charged adsorbent surface and the negatively charged fluoride ions (Zr–F bonds). The adsorbent surface turns negatively charged at basic pH levels. The capacity of fluoride adsorption decreases, as electrostatic

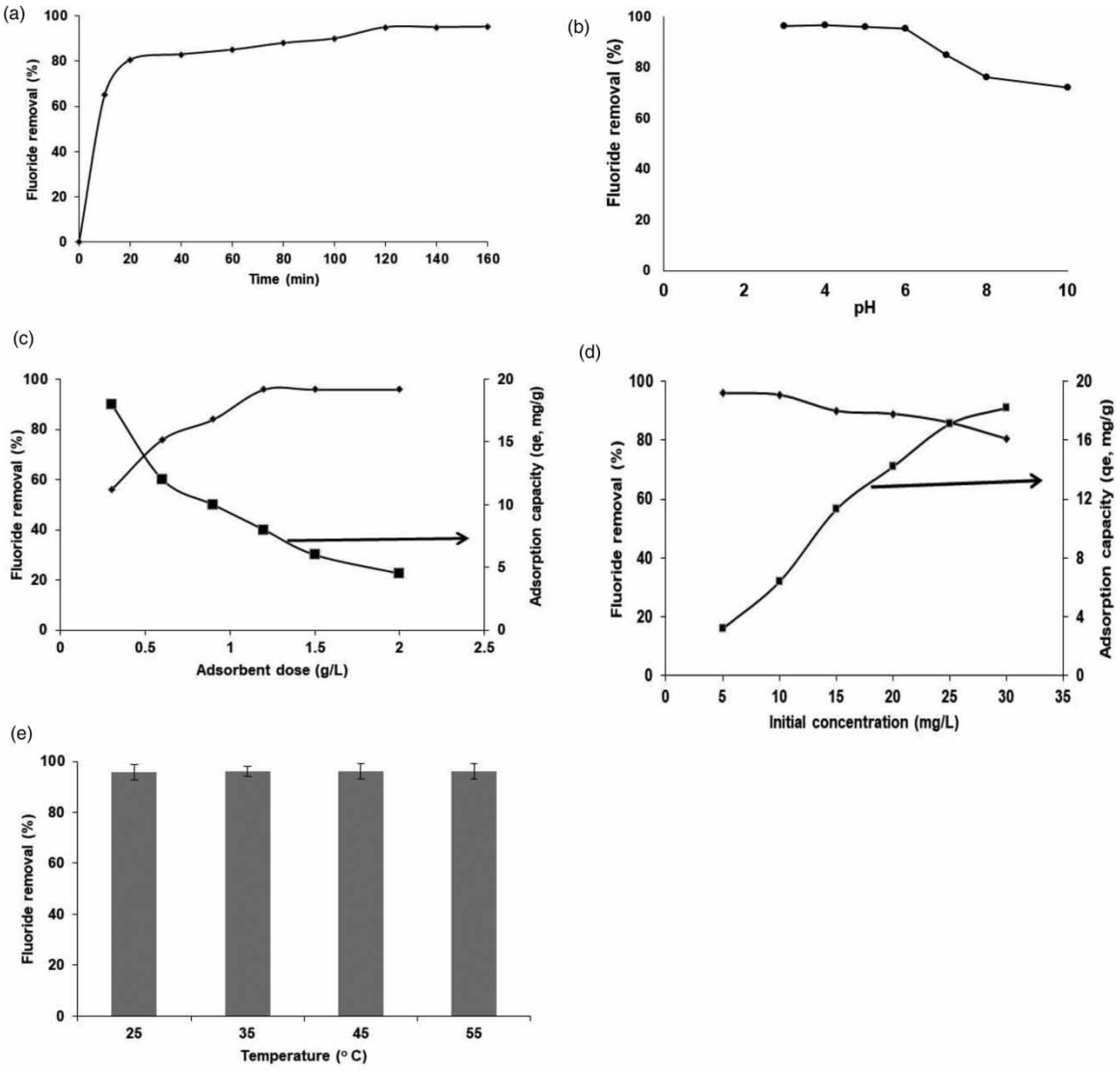

Figure 2 | Fluoride adsorption at different (a) reaction time, (b) pH, (c) adsorbent dose, (d) initial concentration, and (e) temperature.

repulsion between fluoride and adsorbent increases. Data from the literature on the relationship between the zeta potential and pH of ZrFu MOF and hydrous Zr oxide support this result (Dou *et al.* 2012; Ke *et al.* 2018). The effect of the adsorbent dose on fluoride uptake from the synthetic solution was studied with a concentration of 10 mg F/L at an operating condition of $T = 35$ °C, $t = 120$ min, and pH = 6.1. The adsorption capacity, q_e (mg/g), was investigated using MOF doses ranging from 0.3 to 2.0 g/L. The fluoride removal percentage increased from 56 to 96%, with an increased dose from 0.3 to 2.0 g/L of solution. This was due to the availability of the active sites on the adsorbent surface until equilibrium was achieved. Fluoride removal of 96% was achieved at 1 g/L; after that, it remained constant (Figure 2(c)). Correspondingly, the uptake capacity decreased with increased adsorbent dose; this indicates the ratio of fluoride ions available per unit adsorbent decreased with increased loadings. The initial concentration of fluoride in synthetic wastewater varied from 5 to 30 mg/L with an adsorbent dose of 1 g/L, $T = 35$ °C, $t = 120$ min, and pH = 6.1. The fluoride removal efficacy decreased from 98 to 80% with an increased concentration of fluoride in the solution under the operating conditions (Figure 2(d)). At low fluoride concentrations, there were a greater number of adsorption sites available than at higher fluoride concentrations; thus, the adsorption process was rapid. Thus, one of the limiting factors in the adsorption process is the initial concentration of fluoride ions in the solution and the available adsorption sites. The effect of temperature (25, 35, 45, and 55 °C) on fluoride uptake ($C_o = 10$ mg/L, $t = 120$ min, pH = 6.1, adsorbent dose = 1 g/L) was investigated, and it was discovered that above 35 °C, there was no improvement in fluoride uptake (Ke *et al.* 2018). Thus, all the experiments were carried out at 35 °C (Figure 2(e)). The above experimental results were used to calculate the fluoride adsorption isotherms models for Langmuir and Freundlich. The study shows that ZrFu MOF-fluoride adsorption supports the Langmuir monolayer isotherm model compared to the Freundlich multilayer adsorption model (Table 1). The Langmuir separation factor (R_L) was between $0 < R_L < 1$, so the nature of the adsorption process was favourable (Dou *et al.* 2012). The experimentally determined adsorption kinetics indicates that a pseudo-second-order model favours chemisorptions. Similar results were reported earlier (Tan *et al.* 2020).

Table 1 | Study of isothermal constants for fluoride adsorption

Isotherm model	Langmuir	Freundlich
Isotherm parameters	Q_m (mg/g) = 20.10 K_L (L/mg) = 1.24 $R^2 = 0.99$	K_F (mg/g) (L/mg)$^{1/n}$ = 8.78 $n = 2.41$ $R^2 = 0.95$

Similar batch adsorption experiments were conducted with synthetic water at an operating condition ($C_o =$ 150 mg F/L, $T = 35$ °C, pH = 6–7, $t = 60$ min). Figure 3(a) shows that the uptake capacity of ZrFu MOF increased from 37.33 to 100% as the MOF content was increased from 1 to 4.5 g/L. Adsorption equilibrium was reached at 3 g/L ($R = 99.3\%$). The pH of the synthetic water increased from 6.1 to 7.5 after the reaction. This indicates that the mechanism of fluoride uptake by the MOF was ion-exchange, where a fluoride ion replaced the OH ion in the MOF structure. The possible chemical reaction was suggested earlier (Tan *et al.* 2020).

$$Zr - OH + F^- \rightarrow Zr - F + OH^-$$

The high selectivity of ZrFu MOF for fluoride ions was due to the comparatively higher electronegativity and electron-withdrawing property of fluorine compared to halogen elements and oxygen. This results in the replacement of hydroxyl ions by fluoride ions on ZrFu MOF. In addition, the octahedral structure of ZrFu MOF improves the accessibility of the exchange site. It increases diffusion in the entire structure of the MOF, which improves the uptake capacity of the MOF (Tan *et al.* 2020).

A similar study with blast furnace and coke plant wastewater having an initial concentration of 170 and 130 mg/L, respectively, and different contents (2, 3, 4, 6, 8, and 10 g/L) of ZrFu MOF was conducted. More than 90% of fluoride uptake for coke plant wastewater was obtained with 3 g ZrFu/L. Complete uptake was obtained with 10 g ZrFu/L (Figure 3(b)). In a similar study with blast furnace wastewater, 4 g ZrFu/L achieved more than 90% fluoride uptake and 10 g/L achieved complete uptake (Figure 3(c)). Both of these reactions were

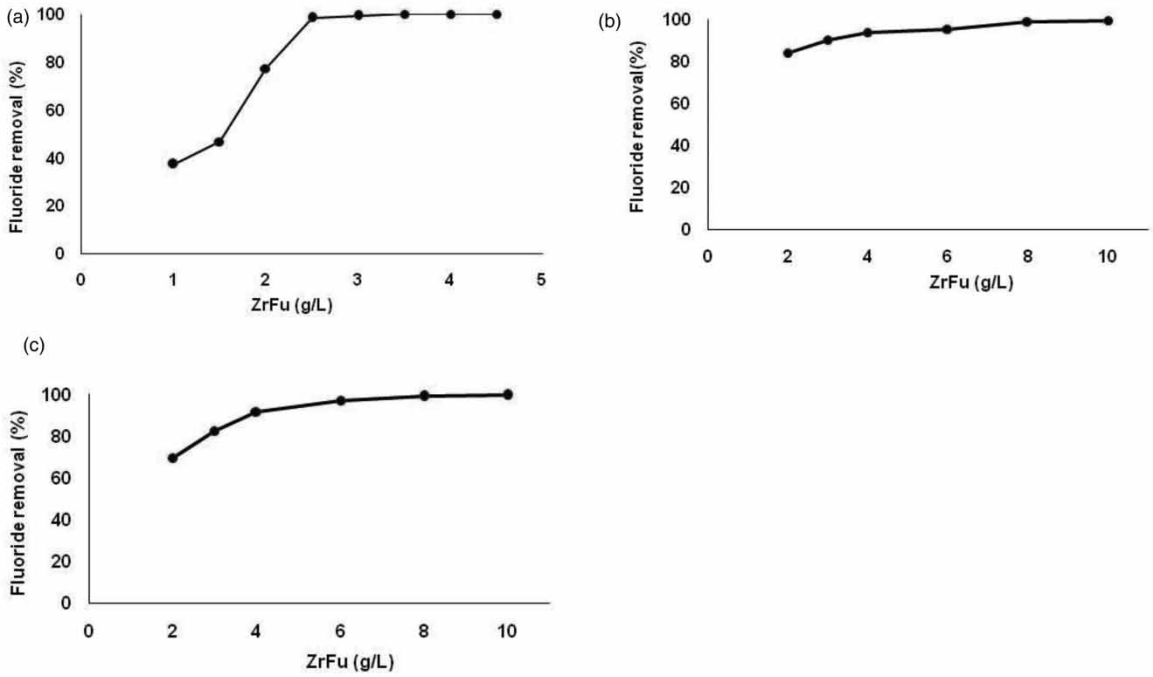

Figure 3 | Fluoride uptake capacity (%) of ZrFu MOF at different adsorbent dose in (a) synthetic water, (b) coke plant, and (c) blast furnace wastewater.

carried out for 60 min. While optimizing the reaction time, almost complete fluoride uptake was obtained within 5 min of the reaction, with 10 g ZrFu/L for the wastewater studied. This shows that the reaction with ZrFu MOF was rapid, indicating the presence of many active sites, which help quick fluoride uptake from wastewater. The wastewater characteristics of the coke plant and blast furnace show that the concentration of fluoride competing ions (Cl^-, PO_4^{3-}, HCO_3^-, NO_3^-) was high for comparable active sites (Table 2). The concentration of coexisting anions before and after the adsorption with ZrFu MOF in coke plant and blast furnace wastewater was studied. Interestingly, after the adsorption process, only phosphate concentration was reduced in coke plant and blast furnace wastewater. This indicates that ZrFu MOF selectively adsorbs fluoride from the solution, and phosphate competes with fluoride for the same active site. Similar observations were reported earlier (Ke *et al.* 2018).

Table 2 | Characteristic of coke plant and blast furnace wastewater before and after adsorption process

Characteristics	Coke plant (as-received)	Coke plant (after adsorption)	Blast furnace (as-received)	Blast furnace (after adsorption)
Fluoride (mg/L)	130 ± 2	0.6 ± 0.1	170 ± 2	1 ± 0.2
Chloride (mg/L)	1,350 ± 2	1,349.6 ± 2	1,799 ± 2	1,796.4 ± 1
Phosphate (mg/L)	7.45 ± 1	2.13 ± 1	5.85 ± 1	2.57 ± 1
Nitrate (mg/L)	10.64 ± 1	10.62 ± 2	11.9 ± 2	11.6 ± 2
Total hardness (mg/L $CaCO_3$)	59 ± 1	60 ± 2	39.6 ± 2	42 ± 1
pH	7.3 ± 0.2	7.7 ± 0.3	7.1 ± 0.1	7.6 ± 0.2

The pH_{zpc} of hydrous zirconium oxide was 6.7 (Dou *et al.* 2012). In the present study, ZrFu MOF was protonated when the solution pH was less than 6.7 and deprotonated when the solution pH was above 6.7 (Figure 4(a) and 4(b)). Protonation allows the breaking of Zr–O bonds, replacing oxygen with fluorine (Figure 4(c)). Figure 5 shows the adsorption peak at 1,425 and 1,602 cm^{-1} before adsorption, which indicates the bending vibration of Zr–OH groups (Dou *et al.* 2012). The peaks have enlarged after adsorption, and the emergence of peaks at 1,056 and 1,139 cm^{-1} shows that fluoride has taken the position of hydroxyl groups. Since the study range was 400 cm^{-1} and beyond, the peaks of the Zr–F stretching and F–Zr–F bending vibrations, which appear around

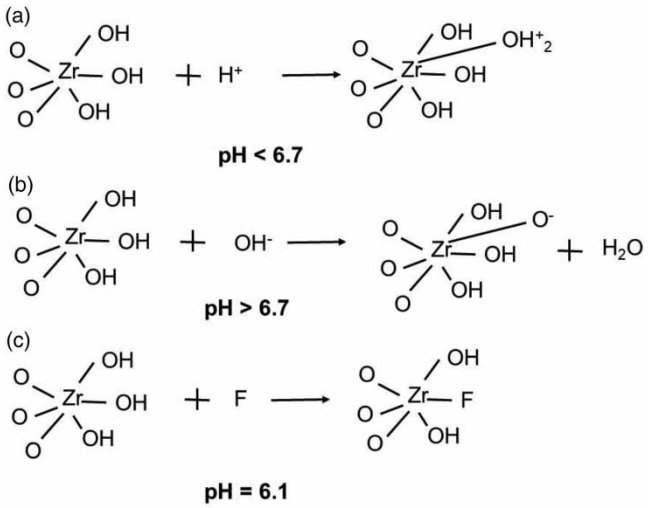

Figure 4 | Possible mechanisms of fluoride adsorption on ZrFu MOF include (a) protonation, (b) deprotonation, and (c) ion-exchange mechanisms.

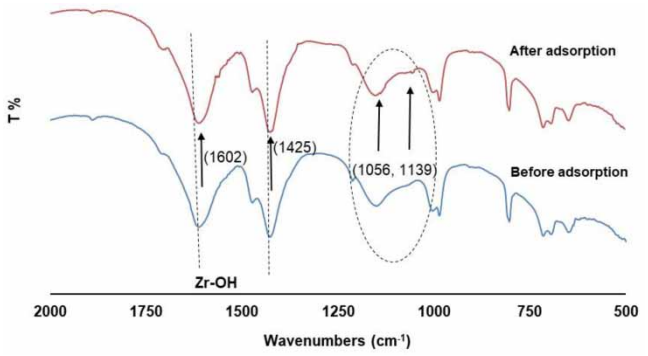

Figure 5 | FTIR spectra before and after fluoride adsorption.

375–475 cm^{-1} and 250–350 cm^{-1}, respectively, were not seen. A comparative study of the performance of different MOFs reported for fluoride removal from water indicates that the uptake capacity of the MOFs is different due to differences in the morphology and composition of the MOFs. ZrFu MOF in the present study performed much better than other Zr MOFs or Zr-based MOF adsorbents (Supplementary Table S1).

3.3. Recovery of ZrFu MOF

ZrFu MOF (10 g/L) was added to synthetic wastewater (150 mg F/L) and reused several times. Figure 6(a) shows the fluoride adsorption–desorption cycle in synthetic water. For the first three cycles (C1–C3), the fluoride uptake capacity was greater than 90%. After that, it gradually decreased in consecutive cycles of operation, and finally, after the 7th cycle, it reached a steady uptake of 70% until the 10th cycle of operation (C10). Similar experiments were carried out with coke plant (130 mg F/L) and blast furnace (170 mg/L) wastewater, respectively (Figure 6(b) and 6(c)). The fluoride uptake capacity of coke plant wastewater decreased from 99 to 80% after the first adsorption–desorption cycle; the uptake capacity decreased in subsequent cycles until it reached 62% after the fourth cycle and continued until the sixth cycle (C4–C6) (50 mg F/L). Similar results were obtained with blast furnace wastewater, the uptake capacity decreased from 99 to 65% in the 2nd cycle of operation, and after that, it remained constant until the 6th cycle (C2–C6) (60 mg F/L). This indicates that the adsorption–desorption process results in 60–65% fluoride recovery from wastewater even after repeated use. The study shows that the efficacy of MOF regeneration decreases after each cycle of adsorption–desorption; this could be due to the strong chemical bonding between ZrFu MOF and fluoride (chemisorption process), which decreases the regeneration efficiency.

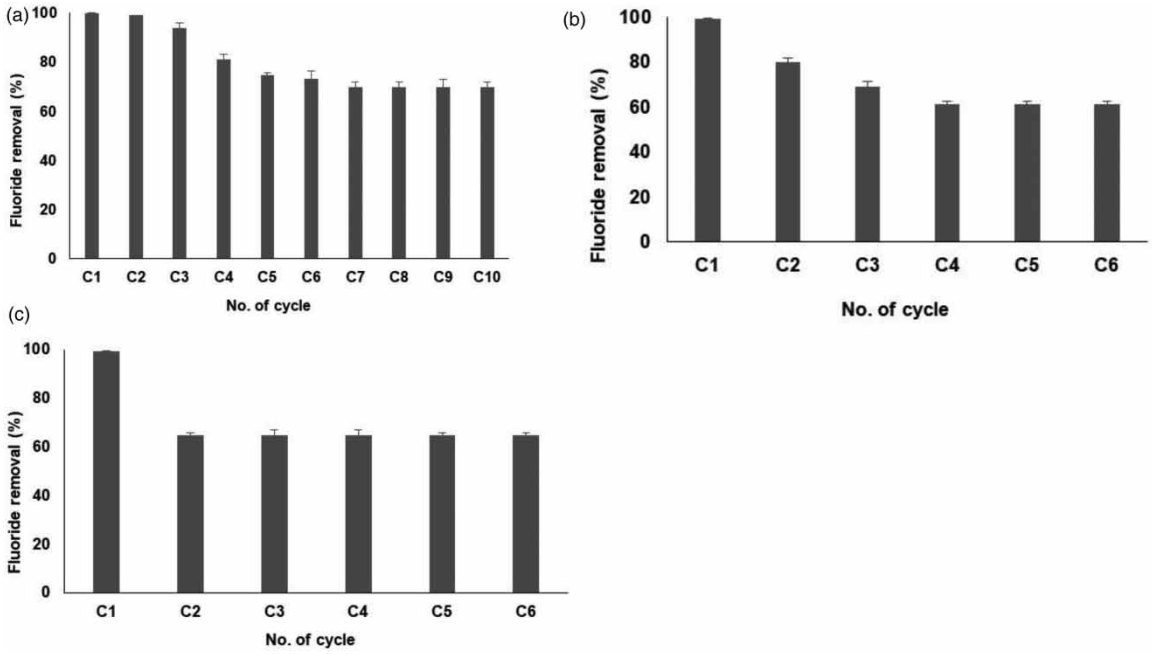

Figure 6 | Fluoride recovery from (a) synthetic water, (b) coke plant, and (c) blast furnace wastewater following adsorption–desorption cycles.

However, 60–65% recovery of fluoride from wastewater could still be helpful for the industries to recover from the waste stream.

4. CONCLUSIONS

This study reported fluoride recovery from industrial wastewater by adsorption using ZrFu MOF. The morphology, porous structure, and fluoride uptake capacity were studied systematically. Different process parameters showed that the fluoride uptake capacity improved with an increase in MOF addition in the batch reactor and reaction time. Fluoride adsorption followed the Langmuir adsorption isotherm and the pseudo-second-order rate law, according to kinetic studies. ZrFu MOF absorbed fluoride completely from synthetic water, coke plant wastewater, and blast furnace wastewater, with uptake capacities of 49.66, 13, and 17 mg/g, respectively. Because of the high surface area of ZrFu MOF (538 m^2/g), it quickly absorbed fluoride from wastewater and reached adsorption equilibrium. When the solution pH was less than pH_{ZPC}, protonated hydroxyl groups encouraged fluoride attraction to ZrFu MOF. The MOF regeneration studies showed that ZrFu MOF reaches a steady fluoride uptake capacity after repeated adsorption–desorption cycles. This is C7 (70%) for synthetic water, C4 (62%) for coke plants, and C2 (65%) for blast furnace wastewater. This variation was due to (i) a different initial fluoride concentration and (ii) with or without interfering ions at the same adsorption sites in the solution. Thus, fluoride may be recovered on-site through the adsorption column by an adsorption–regeneration cycle operation.

ACKNOWLEDGEMENTS

R.K. acknowledges the Ministry of Education (GoI), for the doctoral fellowship.

DATA AVAILABILITY STATEMENT

All relevant data are included in the paper or its Supplementary Information.

CONFLICT OF INTEREST

The authors declare there is no conflict.

REFERENCES

APHA, AWWA, WEF 1998 *Standard Methods for the Examination of Water and Wastewater, 20th edn. American Public Health Association/American Water Works Association/Water*, Environment Federation, Washington, DC, USA.

Castillo, N. A. M., Briano, S. A. C., Ramos, R. L., Pirajan, J. C. M., Dosal, A. T., Gutierrez, L. G., Delgado, G. J. L., Perez, R. O., Estupinan, J. P. R., Lopez, S. Y. R. & Mendoza, M. S. B. 2020 Use of bone char prepared from an invasive species, pleco fish (*Pterygoplichthys* spp.), to remove fluoride and Cadmium (II) in water. *Journal of Environmental Management* **256**, 109956.

Chang, M. F. & Liu, J. C. 2007 Precipitation removal of fluoride from semiconductor wastewater. *Journal of Environmental Engineering* **133**, 419–425.

DeCoste, J. B. & Peterson, G. W. 2014 Metal-organic frameworks for air purification of toxic chemicals. *Chemical Reviews* **114**, 5695–5727.

Dehghani, M. H., Haghighat, G. A., Yetilmezsoy, K., McKay, G., Heibati, B., Tyagi, I., Agarwal, S. & Gupta, V. K. 2016 Adsorptive removal of fluoride from aqueous solution using single- and multi-walled carbon nanotubes. *Journal of Molecular Liquids* **216**, 401–410.

Dey, S., Goswami, S. & Ghosh, U. C. 2004 Hydrous ferric oxide (HFO) – a scavenger for fluoride from contaminated water. *Water, Air, & Soil Pollution* **158**, 311–323.

Dhanasekaran, P., Sai, P. M. S. & Gnanasekar, K. I. 2017 Fixed bed adsorption of fluoride by *Artocarpus hirsutus* based adsorbent. *Journal of Fluorine Chemistry* **195**, 37–46.

Diwani, G. E., Amin, S. K., Attia, N. K. & Hawash, S. I. 2022 Fluoride pollutants removal from industrial wastewater. *Bulletin of the National Research Centre* **46**, 143–152.

Dou, X., Mohan, D., Pittman, C. U. & Yang, S. 2012 Remediating fluoride from water using hydrous zirconium oxide. *Chemical Engineering Journal* **198–199**, 236–245.

Drouiche, N., Ghaffour, N., Lounici, H. & Mameri, M. 2007 Electrocoagulation of chemical mechanical polishing wastewater. *Desalination* **214**, 31–37.

Drouiche, N., Aoudj, S., Lounici, H., Mahmoudi, H., Ghaffour, N. & Goosen, M. F. A. 2012 Development of an empirical model for fluoride removal from photovoltaic wastewater by electrocoagulation process. *Desalination and Water Treatment* **29**, 96–102.

Eddaoudi, M., Kim, J., Rosi, N., Vodak, D., Wachter, J., O'Keeffe, M. & Yaghi, O. M. 2002 Systematic design of pore size and functionality in isoreticular MOFs and their application in methane storage. *Science* **295**(5554), 469–472.

Ezzeddine, A., Meftah, N. & Hannachi, A. 2015 Removal of fluoride from an industrial wastewater by a hybrid process combining precipitation and reverse osmosis. *Desalination and Water Treatment* **55**, 2618–2625.

Furukawa, H., Cordova, K. E., O'Keeffe, M. & Yaghi, O. M. 2013 The chemistry and applications of metal-organic frameworks. *Science* **341**(6149), 1230444.

Halla, V. J. L., Esmeralda, V. A., Luis, F. A. J., Horacio, F. Z. & Rene, R. M. J. 2015 Water defluoridation with special emphasis on adsorbents-containing metal oxides and/or hydroxides: a review. *Separation and Purification Technology* **150**, 292–307.

Jeyaseelan, A., Naushad, M. & Viswanathan, N. 2020 Development of multivalent metal-ion-fabricated fumaric acid-based metal-organic frameworks for defluoridation of water. *Journal of Chemical Engineering Data* **65**(6), 2990–3001.

Jeyaseelan, A., Kumar, I. A., Viswanathan, N. & Naushad, M. 2022 Development and characterization of hydroxyapatite layered lanthanum organic frameworks by template method for defluoridation of water. *Journal of Colloid and Interface Science* **622**, 228–238.

Jung, K. W., Hwang, M. J., Jeong, T. U., Chau, D. M., Kim, K. & Ahn, K. H. 2016 Entrapment of powdered drinking water treatment residues in calcium-alginate beads for fluoride removal from actual industrial wastewater. *Journal of Industrial and Engineering Chemistry* **39**, 101–111.

Karmakar, S., Dechnik, J., Janiak, C. & De, S. 2016 Aluminium fumarate metal-organic framework: a super adsorbent for fluoride from water. *Journal of Hazardous Materials* **303**, 10–20.

Ke, F., Peng, C., Zhang, T., Zhang, M., Zhou, C., Cai, H., Zhu, J. & Wan, X. 2018 Fumarate-based metal-organic frameworks as a new platform for highly selective removal of fluoride from brick tea. *Scientific Reports* **8**, 1–11.

Khatibikamal, V., Torabian, A., Janpoor, F. & Hoshyaripour, G. 2010 Fluoride removal from industrial wastewater using electrocoagulation and its adsorption kinetics. *Journal of Hazardous Materials* **179**, 276–280.

Kumari, U., Behra, S. K. & Meikap, B. C. 2019 A novel acid modified alumina adsorbent with enhanced defluoridation property: kinetics, isotherm study and applicability on industrial wastewater. *Journal of Hazardous Materials* **365**, 868–882.

Kumari, U., Siddiqi, H., Bal, M. & Meikap, B. C. 2020 Calcium and zirconium modified acid activated alumina for adsorptive removal of fluoride: performance evaluation, kinetics, isotherm, characterization and industrial wastewater treatment. *Advanced Powder Technology* **31**, 2045–2060.

Kumari, R., Kumar, A. & Basu, S. 2022 Aluminium fumarate-based polymer matrix composite for selective removal of fluoride from ground water. *Environmental Nanotechnology, Monitoring & Management* **17**, 100642.

Li, J. R., Ma, Y., McCarthy, M. C., Sculley, J., Yu, J., Jeong, H.-K., Balbuena, P. B. & Zhou, H. C. 2011 Carbon dioxide capture-related gas adsorption and separation in metal-organic frameworks. *Coordination Chemistry Reviews* **255**, 1791–1823.

Li, Y., Yang, Y., Qu, G., Ren, Y., Wang, Z., Ning, P., Wu, F. & Chen, X. 2022 Reuse of secondary aluminum ash: study on removal of fluoride from industrial wastewater by mesoporous alumina modified with citric acid. *Environmental Technology & Innovation* **28**, 102868.

Loganathan, P., Vigneswaran, S., Kandasamy, J. & Naidu, R. 2013 Defluoridation of drinking water using adsorption processes. *Journal of Hazardous Materials* **248–249**, 1–19.

Ma, S. & Zhou, H. C. 2010 Gas storage in porous metal-organic frameworks for clean energy applications. *RSC - Chemical Communications* **46**, 44–53.

Meenakshi, M. R. C. 2006 Fluoride in drinking water and its removal. *Journal of Hazardous Materials* **137**, 456–463.

Melidis, P. 2015 Fluoride removal from aluminium finishing wastewater by hydroxyapatite. *Environmental Processes* **2**, 205–213.

Menad, N., Ayala, J. N., Carcedo, F. G., Ayucar, E. R. & Hernandez, A. 2003 Study of the presence of fluorine in the recycled fractions during carbothermal treatment of EAF dust. *Waste Management* **23**, 483–491.

Mohapatra, M., Anand, S., Mishra, B. K., Giles, D. E. & Singh, P. 2009 Review of fluoride removal from drinking water. *Journal of Environmental Management* **91**, 67–77.

Mukherjee, R., Mondal, M., Sinha, A., Sarkar, S. & De, S. 2016 Application of nanofiltration membrane for treatment of chloride rich steel plant effluent. *Journal of Environmental Chemical Engineering* **4**, 1–9.

Patel, S. B., Swain, S. K., Jha, U., Patnaik, T. & Dey, R. K. 2016 Development of new zirconium loaded shellac for defluoridation of drinking water: investigations of kinetics, thermodynamics and mechanistic aspects. *Journal of Environmental Chemical Engineering* **4**, 4263–4274.

Qiu, Y., Ren, L. F., Xia, L., Shao, J., Zhao, Y. & Bruggen, B. V. 2022 Investigation of fluoride and silica removal from semiconductor wastewater with a clean coagulation-ultrafiltration process. *Chemical Engineering Journal* **438**, 135562.

Shan, Y. & Guo, H. 2013 Fluoride adsorption on modified natural siderite: optimization and performance. *Chemical Engineering Journal* **223**, 183–191.

Singh, K., Lataye, D. H., Wasewar, K. L. & Yoo, C. K. 2013 Removal of fluoride from aqueous solution: status and techniques. *Desalination and Water Treatment* **51**, 3233–3247.

Tan, T. L., Krusnamurthy, P. A/P., Nakajima, H. & Rashid, S. A. 2020 Adsorptive, kinetics and regeneration studies of fluoride removal from water using zirconium-based metal organic frameworks. *Royal Society of Chemistry Advances* **10**, 18740.

Waghmare, S. S. & Arfin, T. 2015 Fluoride removal from water by various techniques: review. *International Journal of Innovative Science, Engineering & Technology* **2**, 560–571.

Wan, K., Huang, L., Yan, J., Ma, B., Huang, X., Luo, Z., Zhang, H. & Xiao, T. 2021 Removal of fluoride from industrial wastewater by using different adsorbents: a review. *Science of the Total Environment* **773**, 145535.

Wu, T., Mao, L. & Wang, H. 2017 Adsorption of fluoride from aqueous solution by using hybrid adsorbent fabricated with Mg/Fe composite oxide and alginate via a facile method. *Journal of Fluorine Chemistry* **200**, 8–17.

Zhang, N., Yang, X., Yu, X., Jia, Y., Wang, J., Kong, L., Jin, Z., Sun, B., Luo, T. & Liu, J. 2014 Al-1,3,5-benzenetricarboxylic metal-organic frameworks: a promising adsorbent for defluoridation of water with pH insensitivity and low aluminium residual. *Chemical Engineering Journal* **252**, 220–229.

Zhu, X. H., Yang, C. X. & Yan, X. P. 2018 Metal-organic framework-801 for efficient removal of fluoride from water. *Microporous Mesoporous Materials* **259**, 163–170.

Zueva, S. B., Ferella, F., Taglieri, G., Michelis, I. D., Pugacheva, I. & Veglio, F. 2020 Zero-liquid discharge treatment of wastewater from a fertilizer factory. *Sustainability* **12**(1), 397–410.

First received 26 October 2022; accepted in revised form 13 April 2023. Available online 28 April 2023